Rapid Detection of Track Changes from Onboard Data Acquisition Records: Year 2

Dimitris Rizos, Ph.D.
Professor of Civil Engineering & Environmental Engineering
Molinaroli College of Engineering and Computing
University of South Carolina (USC)

Reza Naseri
PhD Candidate
Molinaroli College of Engineering and Computing
University of South Carolina (USC)

A Report on Research Sponsored by

University Transportation Center for Railway Safety (UTCRS)

Molinaroli College of Engineering and Computing
University of South Carolina (USC)

December 2025

Technical Report Documentation Page

<table>
<tr><td colspan="2">1. Report No.
UTCRS-USC-I7CY24</td><td colspan="2">2. Government Accession No.</td><td colspan="2">3. Recipient's Catalog No.</td></tr>
<tr><td colspan="4" rowspan="2">4. Title and Subtitle
Rapid Detection of Track Changes from Onboard Data Acquisition Records: Year 2</td><td colspan="2">5. Report Date
December 31, 2025</td></tr>
<tr><td colspan="2">6. Performing Organization Code
UTCRS-USC</td></tr>
<tr><td colspan="4">7. Author(s)
Dimitris Rizos, and Reza Naseri</td><td colspan="2">8. Performing Organization Report No.
UTCRS-USC-I7CY24</td></tr>
<tr><td colspan="4" rowspan="2">9. Performing Organization Name and Address
University Transportation Center for Railway Safety (UTCRS)
University of South Carolina (USC)
Columbia, SC 29208</td><td colspan="2">10. Work Unit No. (TRAIS)</td></tr>
<tr><td colspan="2">11. Contract or Grant No.
69A3552348340</td></tr>
<tr><td colspan="4" rowspan="2">12. Sponsoring Agency Name and Address
U.S. Department of Transportation (USDOT)
University Transportation Centers Program
1200 New Jersey Ave. SE
Washington, DC, 20590</td><td colspan="2">13. Type of Report and Period Covered
June 1, 2024 - August 31, 2025</td></tr>
<tr><td colspan="2">14. Sponsoring Agency Code
USDOT UTC Program</td></tr>
<tr><td colspan="6">15. Supplementary Notes</td></tr>
<tr><td colspan="6">16. Abstract
This report presents Year-2 progress toward the development of a scalable, onboard framework for the rapid detection of track changes using in-motion data acquisition records from rail vehicles. Building on the feasibility study established in Year-1, the proposed approach integrates a multi-stage, physics-informed signal-processing framework to extract stiffness-sensitive features from nonstationary onboard vibration measurements. Rather than estimating absolute stiffness, the method adopts a change-based detection strategy using instantaneous energy metrics derived from vertical acceleration data. Year-2 activities focused on evaluating feasibility and robustness through high-fidelity three-dimensional vehicle–track interaction simulations and a scaled laboratory experimental platform. Numerical results demonstrated that representative stiffness-deficient conditions produce spatially localized and repeatable energy signatures, while laboratory experiments confirmed consistent detection across multiple vehicle passes under controlled conditions. Collectively, the results establish the technical feasibility of detecting track stiffness changes using onboard measurements without requiring track access or service interruption. These findings provide a foundation for future field validation and advancement toward real-time, network-scale deployment.</td></tr>
<tr><td colspan="3">17. Key Words
Railroad tracks; Stiffness; Accelerometers; Monitoring</td><td colspan="3">18. Distribution Statement
This report is available for download from
https://www.utrgv.edu/railwaysafety/research/infrastructure/index.htm</td></tr>
<tr><td>19. Security Classification (of this report)
None</td><td colspan="2">20. Security Classification (of this page)
None</td><td colspan="2">21. No. of Pages
30</td><td>22. Price</td></tr>
</table>

Table of Contents

List of Figures

List of Tables

List of Abbreviations

Abbreviation	Definition
FRA	Federal Railroad Administration
HT	Hilbert Transform
IMF	Intrinsic Mode Function
PTT	Precision Test Track
SNR	Signal to Noise Ratio
TGI	Track Geometry Irregularities
TSI	Track Stiffness Irregularities
TTC	Technology Testing Center
USDOT	U.S. Department of Transportation
UTC	University Transportation Center
VMD	Variational Mode Decomposition
WPA	Wavelet Packet Analysis

Disclaimer

The contents of this report reflect the views of the authors, who are responsible for the facts and the accuracy of the information presented herein. This document is disseminated under the sponsorship of the U.S. Department of Transportation's University Transportation Centers Program, in the interest of information exchange. The U.S. Government assumes no liability for the contents or use thereof.

Acknowledgements

The authors wish to acknowledge the University Transportation Center for Railway Safety (UTCRS) for funding this project under the USDOT UTC Program Grant No 69A3552348340.

1 SUMMARY

This report documents Year-2 progress on the development of a scalable, onboard framework for the rapid detection of track stiffness changes using in-motion vibration measurements collected from in-service rail vehicles. The work builds on the foundational feasibility demonstrated in Year-1 and advances the methodology through more realistic numerical modeling and controlled experimental validation. The proposed approach integrates a multi-stage, physics-informed signal-processing framework to extract stiffness-sensitive features from nonstationary onboard acceleration data. Rather than estimating absolute stiffness values, the method adopts a change-based detection paradigm, in which localized deviations in dynamic response are identified using instantaneous energy metrics derived from vertical vibration measurements. Year-2 activities focused on evaluating the feasibility and robustness of the proposed framework using two complementary validation platforms: a high-fidelity numerical simulation and a scaled physical experiment. First, a high-fidelity three-dimensional (3D) vehicle–track interaction simulation was employed to assess performance under realistic vehicle dynamics, distributed track support conditions, and measured track geometry inputs. The simulations demonstrated that stiffness deficiencies associated with excessive deflection, abrupt sleeper-to-sleeper stiffness transitions, and non-compliant stiffness ranges produce consistent and spatially localized signatures in the instantaneous energy domain. Second, a scaled laboratory experimental platform was developed to enable repeatable testing in a physically controlled environment. The laboratory experiments confirmed that stiffness-induced dynamic signatures can be consistently identified across multiple vehicle passes and under continuous operation. Repeated traversal of stiffened track segments produced reproducible changes in instantaneous energy aligned with known support conditions, supporting the robustness of the proposed detection approach.

Collectively, the Year-2 results demonstrate the technical feasibility of detecting track stiffness changes using onboard vibration data without requiring track access or service interruption. While the work remains at a proof-of-concept and feasibility level, the findings establish a strong foundation for subsequent field validation, refinement of classification and severity assessment, and progression toward real-time, edge-compatible deployment. These advancements support the long-term goal of enabling network-scale, data-driven track condition monitoring to inform proactive maintenance and enhance railway safety.

2 BACKGROUND

Railway track performance is fundamentally governed by the dynamic interaction between moving vehicles and the compliant track support system. Among track compliance properties, track stiffness plays a critical role in determining load distribution, vibration response, and long-term degradation of track components. Spatial variations in track stiffness, commonly referred to as Track Stiffness Irregularities (TSI), are known to accelerate ballast deterioration, induce differential settlement, increase wheel–rail contact forces, and contribute to the initiation and propagation of both track geometry irregularities and rail defects [1-3]. Consequently, reliable detection of track stiffness changes is essential for maintaining safe and efficient rail operations.

Despite its importance, track stiffness monitoring remains far less developed than track geometry inspection. Traditional inspection regimes emphasize geometric indicators such as alignment, profile, and cross-level, while stiffness-related issues are often identified only after significant deterioration has occurred [4, 5]. This limitation is particularly concerning given that stiffness irregularities frequently precede observable geometric defects and may remain undetected until the track is subjected to repeated dynamic loading under in-service trains.

2.1 Track Stiffness and Its Dynamic Nature

Track stiffness is commonly defined as the resistance of the rail–track system to vertical deformation under load and is influenced by multiple components, including rail pads, sleepers, ballast, subgrade, and fastening systems. Classical approaches to stiffness characterization rely on static or quasi-static measurements, typically obtained by applying known loads and measuring rail deflection [6-8]. While such methods provide valuable insight into average support conditions, they do not fully capture the dynamic behavior of the track under moving loads, nor do they reflect the actual conditions experienced during train operation.

Under real operating conditions, trains impose time-varying, dynamic loads that excite the coupled vehicle–track system across a wide range of frequencies. The resulting dynamic stiffness differs from static stiffness and is strongly affected by inertial effects, damping, and nonlinear contact behavior [9, 10]. Research has shown that even small localized stiffness changes can significantly alter the dynamic response of the vehicle–track system, leading to amplified accelerations, increased wheel unloading, and higher impact forces at stiffness transition zones [2, 11]. These effects are particularly pronounced near bridge approaches, degraded ballast regions, unsupported sleepers, and areas with subgrade variability [3, 5].

2.2 Limitations of Existing Track Stiffness Monitoring Methods

Existing techniques for measuring track stiffness can be broadly classified into spot-checking methods and specialized inspection vehicle systems. Spot-checking approaches, such as jack-loading tests, falling weight deflectometers, and impact hammer measurements, require direct access to the track and often necessitate traffic interruptions [12, 13]. While these methods can provide accurate localized measurements, they are labor-intensive, slow, and impractical for network-wide deployment.

Specialized inspection vehicles equipped with dedicated sensors offer improved coverage but come with substantial operational and financial costs [14-16]. Their infrequent deployment limits temporal resolution, making it difficult to detect emerging stiffness changes before they evolve into critical defects. Moreover, many of these systems rely on controlled test conditions and are not designed to operate continuously under revenue service.

As a result, current practice faces a fundamental trade-off between measurement accuracy, spatial coverage, temporal resolution, and cost, leaving a critical gap in the ability to perform scalable, continuous stiffness monitoring across large rail networks [1, 3].

2.3 In-Motion and Onboard Monitoring as a Scalable Alternative

Recent advances in sensing technology, data acquisition, and signal processing have created new opportunities for in-motion track condition monitoring using onboard measurements. By installing sensors directly on in-service vehicles, it becomes possible to collect vibration data during normal operation without disrupting service [14, 17]. This approach offers several key advantages: frequent data collection, broad spatial coverage, reduced reliance on dedicated inspection vehicles, and the ability to observe the track under realistic loading conditions.

Vertical acceleration measurements recorded from bogies or axle boxes are particularly sensitive to changes in track support conditions [18, 19] . However, these signals are inherently nonstationary, nonlinear, and contaminated by operational variability, including speed fluctuations, vehicle dynamics, and environmental noise [3]. Extracting stiffness-related information from such data therefore requires advanced signal processing techniques capable of isolating subtle, localized changes while remaining computationally efficient.

2.4 Multi-Stage Physics-Informed Signal Processing for Track Change Detection

To address these challenges, the proposed research builds upon a multi-stage physics-informed signal processing framework that integrates complementary time–frequency and energy-based methods [20]. The underlying premise is that changes in track stiffness manifest as localized alterations in the energy distribution and instantaneous frequency content of onboard vibration signals [21, 22]. By combining multi-resolution decomposition techniques with adaptive, data-driven analysis, the framework enhances sensitivity to stiffness changes while maintaining robustness to noise and operational variability.

Unlike conventional frequency-domain approaches that assume stationarity, the proposed framework is specifically designed to operate on short data windows and capture transient responses associated with localized stiffness changes. This makes it well suited for edge-compatible, near-real-time implementation, a key requirement for scalable deployment on in-service trains.

2.5 Progress Beyond Year-1 and Motivation for Year-2 Research

The Year-1 phase of this research established the initial feasibility of detecting track stiffness changes from onboard acceleration records using a Wavelet–Hilbert-based approach [20]. Numerical simulations demonstrated that stiffness changes could be reliably identified through instantaneous energy metrics derived from filtered vibration signals. Building on this foundation, the Year-2 effort expands the scope and rigor of the investigation by:

- Refining the physics-informed signal processing framework [21, 23],
- Evaluating robustness across a broader range of stiffness change scenarios[22],
- Incorporating higher-fidelity vehicle–track interaction modeling [22], and
- Advancing laboratory-scale validation to bridge the gap between numerical feasibility and real-world deployment [24].

This progression directly supports the long-term objective of developing a scalable, onboard system for rapid detection of track changes, aligned with the Federal Railroad Administration's vision for predictive, data-driven rail infrastructure management [25].

3 METHODOLOGY

3.1 Methodology Overview

The proposed methodology enables rapid, in-motion detection of track stiffness irregularities (TSI) using onboard vibration measurements collected from in-service rail vehicles. The approach is based on a multi-stage, physics-informed signal processing framework designed to extract stiffness-sensitive features from nonstationary acceleration signals while remaining computationally efficient and suitable for edge-based implementation. As shown in **Figure 1**, the framework consists of three modules:

1. Data Acquisition,
2. Change Detection, and
3. Change Classification.

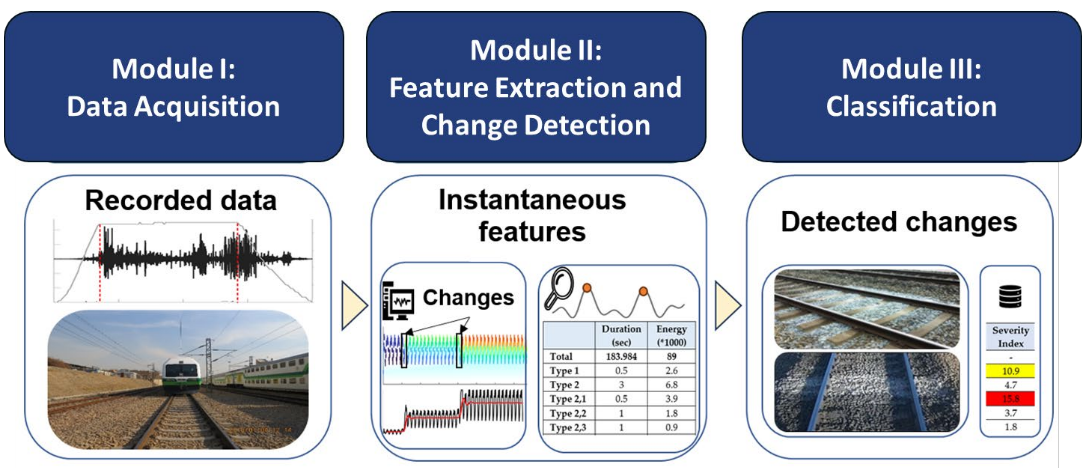

Figure 1: Schematic of sensor positioning system for in-motion data acquisition

This report focuses on the methodological development of the Change Detection module, which forms the analytical core of the system and establishes the feasibility of using instantaneous energy as a proxy for track stiffness variation.

3.2 Module I: Onboard Data Acquisition

Vertical acceleration measurements are collected using bogie-mounted accelerometers, as shown in **Figure 2**, selected to provide a mechanically robust sensing location that captures vehicle–track interaction dynamics while avoiding excessive wheel–rail contact noise. Bogie-level acceleration preserves sensitivity to localized stiffness variations while providing improved signal stability compared to axle-level measurements.

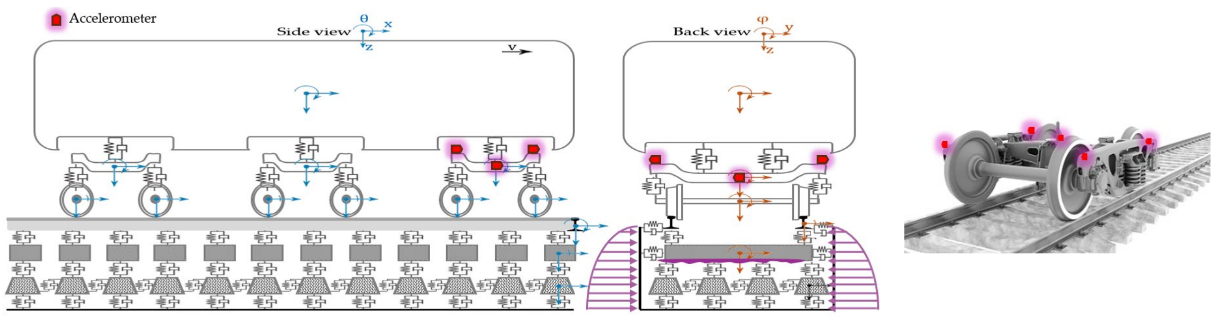

Figure 2: Schematic of sensor positioning system for in-motion data acquisition

Acceleration data are synchronized with train speed and positional information (e.g., GPS or odometry) to enable spatial alignment of detected features along the track. Although near-constant speed is preferred to simplify interpretation, the framework is designed to tolerate realistic operational speed variations, which are addressed through subsequent signal processing stages.

3.3 Module II: Change Detection Framework

The Change Detection module integrates Wavelet Packet Analysis (WPA), Variational Mode Decomposition (VMD), and Hilbert Transform (HT) to isolate stiffness-related vibration signatures and convert them into a spatially distributed energy-based indicator. More details are available in [21, 26, 27].

3.3.1 Wavelet Packet Analysis (WPA)

WPA is employed as the first stage to decompose the measured acceleration signal into frequency-localized components and suppress broadband noise. The wavelet packet basis function is defined as [21]:

$$\psi_{j,k}^{i}(t) = \sqrt{2^j}\,\psi^i(2^j t - k) \qquad (1)$$

where j is the scale level, k is the translation index, and i denotes the modulation index.

For a signal sampled at frequency f_s, the maximum decomposition level is selected as:

$$DL_{\max} = \log_2(\frac{f_s}{f_{\min}}) \qquad (2)$$

The wavelet packet coefficients are computed as:

$$c_{j,k}^i(t) = \int_{-\infty}^{\infty} y(t)\, \psi_{j,k}^i(t)\, dt \qquad (3)$$

Noise reduction is achieved through hard thresholding:

$$\tilde{c}_{j,k}(t) = \begin{cases} c_{j,k}(t), & |\, c_{j,k} \,| \geq \lambda \\ 0, & \text{otherwise} \end{cases} \qquad (4)$$

where the threshold $\lambda = \sigma\sqrt{2\ln\, N}$, following Donoho's formulation, with σ estimated from the median absolute deviation of coefficients.

The denoised signal is reconstructed as:

$$\tilde{y}_j^i(t) = \sum_{k=-\infty}^{\infty} \tilde{c}_{j,k}^i(t)\, \psi_{j,k}^i(t) \qquad (5)$$

This step yields substantial data compaction (>95%) while preserving stiffness-sensitive dynamics.

3.3.2 Variational Mode Decomposition (VMD)

The reconstructed signal is further decomposed using VMD to isolate narrow-band oscillatory modes associated with track support conditions. VMD formulates signal decomposition as the solution to the following constrained variational problem:

$$\min_{\{IMF_i\},\{\omega_i\}} \left\{ \sum_{i=1}^{K} \| \partial_t[(\delta(t) + \frac{j}{\pi t}) * IMF_i(t)]e^{-j\omega_i t} \|_2^2] \right\} \qquad (6)$$

where $IMF_i(t)$ denotes the i-th intrinsic mode function and ω_i its center frequency.

VMD enables robust separation of stiffness-related vibration components from vehicle-specific or roughness-induced effects without assuming signal stationarity.

3.3.3 Hilbert Transform and Instantaneous Energy

Each extracted IMF is processed using the Hilbert Transform:

$$H(t) = \frac{1}{\pi} P \int \frac{IMF(\tau)}{t-\tau}\, d\tau \qquad (7)$$

The instantaneous amplitude, phase, and frequency are computed as:

$$a(t) = \sqrt{IMF^2(t) + H^2(t)} \qquad (8)$$

$$\theta(t) = \tan^{-1}\left(\frac{H(t)}{IMF(t)}\right) \qquad (9)$$

$$\omega(t) = \frac{d\theta(t)}{dt} \qquad (10)$$

The instantaneous energy, used as the primary stiffness proxy, is defined as:

$$IE(\omega, t) = \int H^2(\omega, t)\, d\omega \qquad (11)$$

with the Hilbert amplitude spectrum given by:

$$H(\omega, t) = \Re\left\{\sum_{j=1}^{n} a_j(t) \exp\left(i \int \omega_j(t)\, dt\right)\right\} \qquad (12)$$

The resulting instantaneous-energy profile is spatially aligned with the train trajectory and highlights localized deviations associated with stiffness changes.

3.3.4 Interpretation Strategy

Rather than estimating absolute stiffness values, the methodology adopts a change-based detection paradigm. Track stiffness irregularities are identified as consistent, spatially repeatable deviations in instantaneous energy across multiple passes. Abrupt stiffness transitions manifest as sharp energy peaks, gradual degradation appears as smooth energy trends, and localized weak zones produce distinct energy drops or spikes over short distances. This interpretation is independent of vehicle-specific parameters and does not require prior knowledge of track structure [23, 26].

3.4 Module III: Classification

Module III focuses on the classification and severity assessment of track stiffness irregularities using the features extracted in Module II. At a high level, this module is intended to translate stiffness-sensitive indicators, such as instantaneous energy and related dynamic features, into actionable information regarding the presence, location, and relative severity of track changes. The development, training, and validation of classification and severity models are beyond the scope of the current Year-2 project and are planned as a core component of the proposed Year-3 research effort.

4 EXPERIMENTS

This section presents the experimental evaluation framework developed to assess the feasibility and robustness of the proposed onboard TSI change detection methodology. Two complementary validation platforms are employed. First, a high-fidelity three-dimensional (3D) vehicle–track interaction simulation is used to examine the algorithm performance under realistic vehicle dynamics, distributed track support conditions, and measured track geometry inputs. Second, a scaled laboratory test rig is introduced to enable controlled, repeatable experimentation that preserves the essential dynamic characteristics of full-scale train–track interaction. The objective is not to deliver a fully optimized system, but to demonstrate proof-of-concept, quantify sensitivity to representative stiffness-deficient scenarios, and establish confidence in the proposed framework prior to large-scale implementation.

4.1 High-Fidelity 3D Vehicle–Track Interaction Simulation

To complement the simplified numerical models presented in the first report [28] and to evaluate the proposed detection framework under more realistic operating conditions, a high-fidelity three-dimensional (3D) vehicle–track interaction simulation was employed. The primary objective of the high-fidelity simulation is to evaluate whether the proposed multi-stage, physics-informed signal-processing framework can reliably detect track stiffness irregularities when subjected to complex vehicle dynamics, spatially distributed track support properties, and realistic excitation sources such as measured track geometry. By explicitly incorporating these effects, the simulation captures critical interactions that are not represented in low-order analytical models. Within the overall validation strategy, this high-fidelity model serves as an intermediate evaluation step between simplified numerical feasibility studies and laboratory-scale experimentation. It provides a controlled but physically representative environment in which detection sensitivity, robustness, and spatial localization capability can be systematically examined prior to transition to scaled experimental testing.

4.1.1 Model Overview and Configuration

The high-fidelity simulation, shown in **Figure 3**, represents a single railway vehicle traveling over a discretized track system with spatially varying stiffness properties [26]. The vehicle model consists of a car body supported by three bogies, each modeled with multiple degrees of freedom to capture vertical translation, pitching, rolling, and suspension dynamics. Each bogie assembly includes wheelsets, primary suspension, and secondary suspension components, resulting in a multi-degree-of-freedom vehicle model capable of reproducing realistic vibration responses. The track structure is modeled using a three-dimensional train–track interaction formulation, in which the rail is represented as a flexible beam supported by discrete spring–damper elements corresponding to rail pads, sleepers, ballast, and subgrade. Track support elements are distributed at sleeper spacing intervals, allowing localized stiffness variations to be introduced in a controlled and spatially explicit manner.

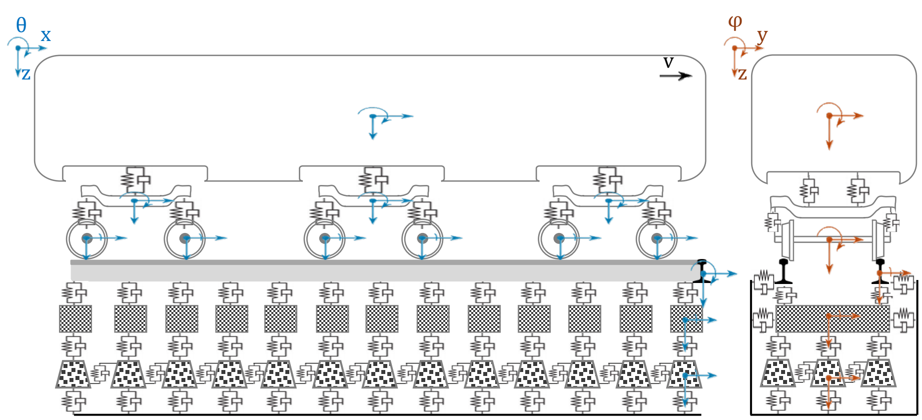

Figure 3: Schematic of the 3D train-track interaction model [26]

4.1.2 *Track Geometry and Stiffness Inputs*

To enhance realism, the vertical track profile was extracted from actual measurements recorded on ballasted tracks using the DOTX 220 inspection vehicle [29]. These data were collected over a segment of the Precision Test Track (PTT) at the FRA's Technology Testing Center (TTC), shown in **Figure 4**. This profile introduces realistic geometric excitation into the model and ensures that the simulated vehicle response reflects both geometric irregularities and stiffness-related effects.

Track stiffness variations are introduced independently of the geometric profile by modifying the stiffness values of selected support elements along the track. This separation allows stiffness irregularities to be examined explicitly without conflating them with geometry defects. To account for operational uncertainty and sensor noise, white Gaussian noise with a signal-to-noise ratio (SNR) of 15 dB was added to the simulated acceleration data. The simulation scenarios were benchmarked against standard railway engineering guidelines as introduced in literature. These include:

a) Maximum allowable vertical deflection: 6.4 mm [30]

b) Acceptable track stiffness range: 50–90 kN/mm (optimal ≈ 75 kN/mm) [4, 31, 32]

c) Sleeper-to-sleeper stiffness variation: less than a factor of 5 [3]

The baseline (intact) model was configured with a uniform stiffness of 78 kN/mm, while three distinct stiffness-deficient cases were designed to evaluate the sensitivity of the proposed detection method under various structural conditions. These scenarios represent conditions associated with ballast degradation, subgrade settlement, and transition zones near rigid structures.

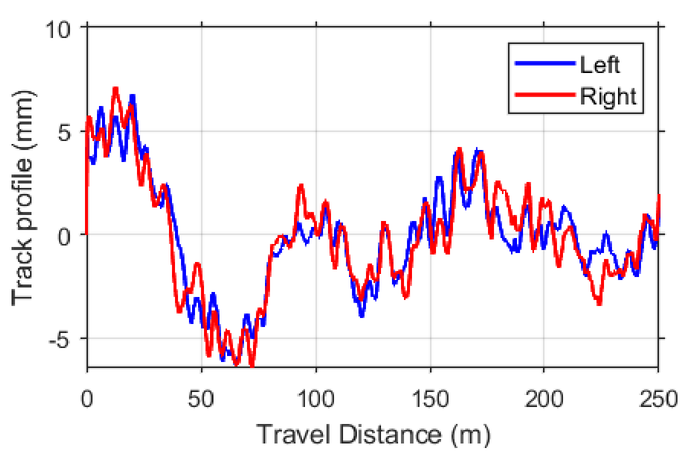

Figure 4: DOTX220 recorded track profile [26]

4.1.3 Simulation Execution and Data Collection

The simulated vehicle traverses a 250-m track segment at a constant speed. Vertical vibration responses are recorded at the middle bogie, which provides a balance between sensitivity to track-induced dynamics and robustness to local wheel–rail contact effects. Acceleration time histories are generated with a sampling rate of 1kHz. To reflect realistic measurement conditions, stochastic noise is added to the simulated signals, ensuring that the resulting dataset resembles operational onboard acceleration records rather than idealized numerical outputs. The simulated acceleration signals are subsequently processed using the proposed signal-processing framework.

4.1.4 Deflection Threshold Analysis

Excessive vertical track deflection is widely recognized as an early indicator of deteriorating support conditions and may precede more severe structural failures. To evaluate the sensitivity of the proposed detection framework to such conditions, a 10-m track segment was modeled with reduced subgrade stiffness to induce vertical deflections exceeding the commonly accepted threshold of 6.4 mm. In the baseline (intact) configuration, a uniform track stiffness of 78 kN/mm resulted in stable vertical deflections of approximately 1.4 mm. In contrast, the deficient configuration produced a peak deflection of 6.6 mm, exceeding the threshold and representing a structurally compromised support condition.

Figure 5 illustrates the variation of the instantaneous energy derived from the vertical bogie acceleration signal for both intact (blue) and deficient (red) track conditions. The left panel presents the energy response over the full track segment, where the intact case exhibits a low and relatively uniform energy level, consistent with stable support conditions. In contrast, the deficient case displays a pronounced and localized increase in energy near 110 m, corresponding to the location of the imposed stiffness reduction. The zoomed-in view shown in the right panel (100–120 m) highlights the detailed response within the deficient region, clearly capturing the onset, peak, and subsequent recovery of the energy signature associated with the localized stiffness loss.

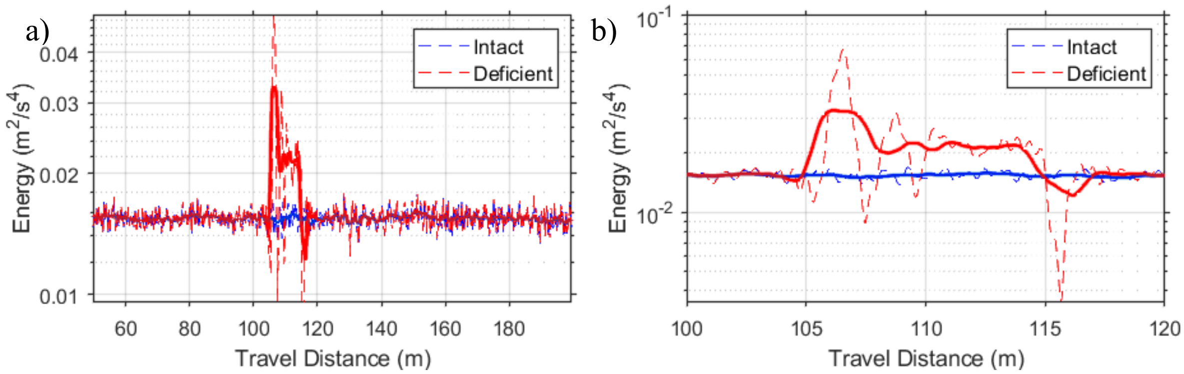

Figure 5: Instantaneous energy response to deflection threshold criteria a) across the full track segment and b) zoomed-in view of the deficient region (100–120 m) [22]

4.1.5 Track Stiffness Ratio Between Adjacent Sleepers

Abrupt changes in stiffness between adjacent sleepers are known to induce localized dynamic amplification and can accelerate track degradation. To evaluate the proposed framework's sensitivity to such conditions, a stiffness discontinuity was introduced between neighboring sleepers by reducing the support stiffness from 75 kN/mm to 15.6 kN/mm, resulting in a stiffness ratio exceeding the commonly referenced threshold value of 5.

Figure 6 illustrates the corresponding response of the instantaneous energy metric extracted from the vertical bogie acceleration signal. The left panel shows the energy variation over the full track segment, where the intact configuration (blue) exhibits a relatively stable response, indicating uniform support conditions. In contrast, the deficient configuration (red) produces a pronounced and spatially localized energy spike at the location of the stiffness discontinuity. The zoomed-in view shown in the right panel (100–120 m) highlights the detailed response near the critical region. A concentrated increase in energy is observed over the affected sleeper length (approximately 1 m), with the elevated response persisting over a distance comparable to the bogie footprint (approximately 2.5 m). This behavior reflects the dynamic influence of the localized stiffness drop on the vehicle–track interaction and demonstrates the framework's capability to identify and spatially resolve sharp stiffness transitions between adjacent support elements.

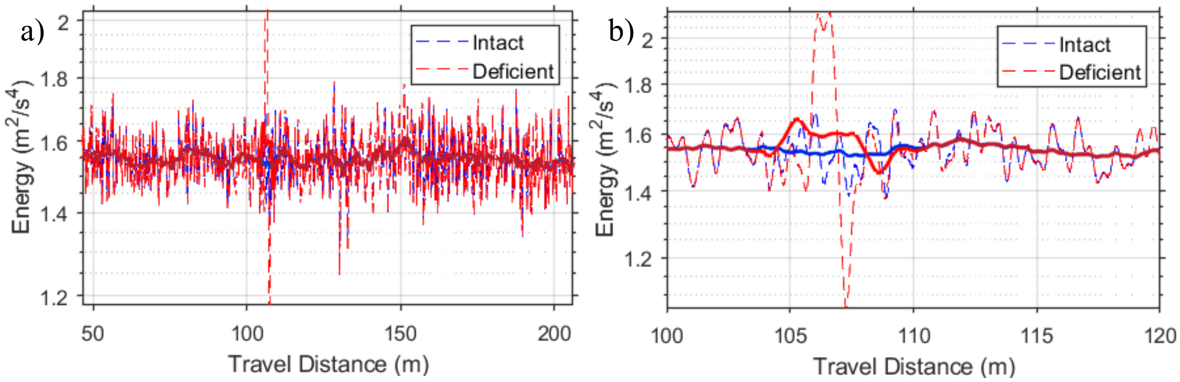

Figure 6: Instantaneous energy response to sleeper-to-sleeper stiffness drop: a) over the full segment b) zoomed-in at the critical location. [22]

4.1.6 Stiffness Range Compliance

This part shows the ability of the proposed framework to identify track stiffness conditions that fall outside the recommended operational range of 50–90 kN/mm. To represent a non-compliant support condition, a 10-m-long track segment with reduced stiffness (k = 30 kN/mm) was introduced into the simulation. The resulting response, shown in **Figure 7**, indicates a clear and sustained increase in the instantaneous energy extracted from the vertical bogie acceleration signal relative to the intact track configuration. While the intact case maintains a comparatively stable and low energy level consistent with compliant support conditions, the deficient segment produces a persistent elevation in energy across the affected region. This sustained response reflects the dynamic influence of prolonged stiffness non-compliance and demonstrates the framework's capability to distinguish track segments with stiffness values outside acceptable operational limits. The results further support the use of instantaneous energy as a robust indicator for identifying stiffness-related support deficiencies under realistic vehicle–track interaction conditions.

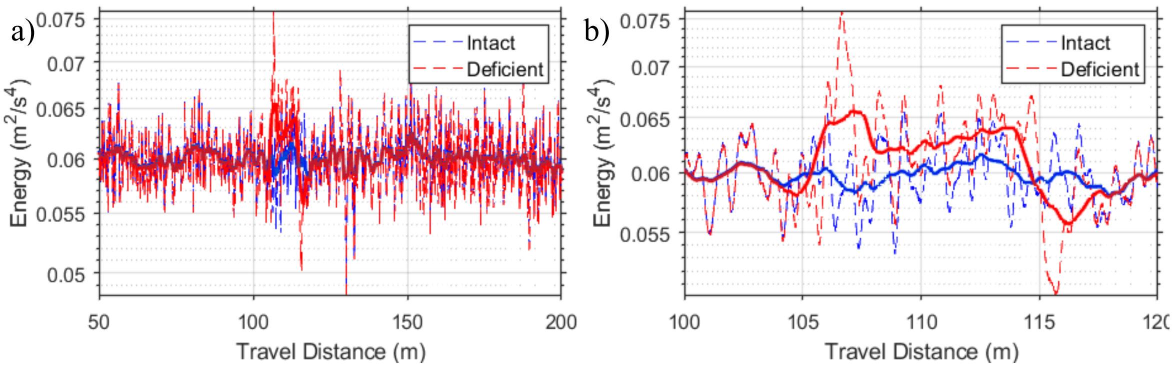

Figure 7: Instantaneous energy response to stiffness range compliance: a) over the full segment b) zoomed-in at the critical location. [22]

4.2 Scaled Laboratory Experimental Platform

While the high-fidelity 3D vehicle–track interaction simulations provide valuable insight into the performance of the proposed detection framework under realistic but idealized conditions, laboratory-scale experimentation is essential to evaluate system behavior in a physically controlled and repeatable environment. In particular, experimental testing allows assessment of sensor response, structural nonlinearity, and operational variability that cannot be fully captured through numerical modeling alone. This section presents the laboratory-scale implementation of the proposed monitoring system, developed to validate the feasibility of detecting track stiffness changes prior to large-scale or field deployment. The scaled test rig is designed to replicate key aspects of track–vehicle interaction using physically meaningful parameters that preserve the dynamic similarity required for vibration-based monitoring. As illustrated in **Figure 8**, the transition from field-observed phenomena to controlled experimental validation begins with interpreting the dominant dynamic mechanisms governing train–track interaction in operational rail systems. These mechanisms are then abstracted into a mechanical design that captures the essential vehicle and track features most sensitive to vertical and lateral dynamics. Following this approach, a small-scale test rig with a 1:28 scaling ratio was developed to reproduce representative dynamic responses within the constraints of a laboratory environment. The lab-scale platform consists of a circular track system, an instrumented vehicle assembly, and a central drive mechanism that enables continuous and repeatable motion. This configuration allows systematic implementation of various track stiffness scenarios—such as localized stiffness reduction, missing support elements, and gradual stiffness transitions—under controlled conditions. Repeated experimental runs can therefore be conducted to generate onboard vibration measurements that are representative of real-world responses, while maintaining full experimental control over system parameters.

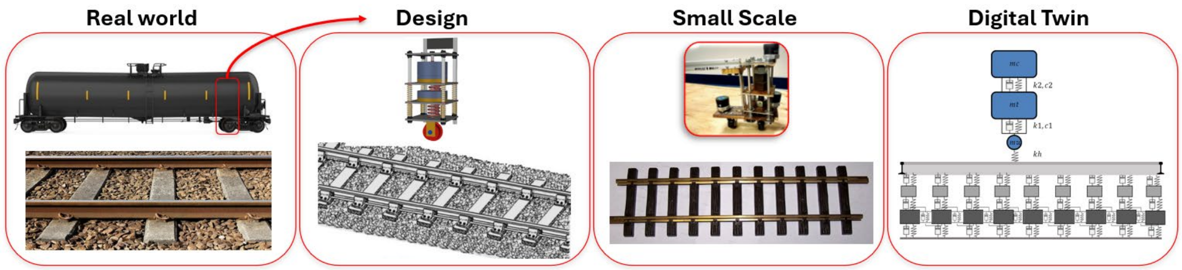

Figure 8: Conceptual overview of the small-scale test rig and its digital twin designed to replicate real-world track conditions

4.2.1 Scaling Strategy

The laboratory test rig operates at a 1:28 scale, chosen to balance laboratory space limitations with the need to accurately replicate the physical and dynamic behavior of the full-scale railway system. This scaling ensures that the critical aspects of vehicle–track interaction, such as vibration transmission, stiffness response, and energy dissipation, are preserved while enabling repeatable experiments under controlled conditions. The scaling factors used in the design of the test rig are summarized in Table 1.

Table 1 Scaling Factors for the Test Rig (N=28)

Parameter	Symbol	Scale Factor	Parameter	Symbol	Scale Factor
Length	*L*	1/N	Damping	C	$1/N^2$
Mass	*M*	$1/N^3$	Frequency	F	N
Force	*F*	$1/N^2$	Acceleration	a	N
Stiffness	*K*	1/N	Stress	σ	1

4.2.2 Setup Components

4.2.2.1 Central Pivot

The central pivot mechanism serves as the drive core of the circular track system, enabling the continuous motion required for extended and repeatable testing. As shown in **Figure 9**, the pivot consists of a vertically mounted motor, a central shaft, and a custom-built support housing. The motor used is a high-torque-low-speed, capable of rotating the drive beam at speeds up to 12 RPM. A belt and pulley system transfers torque from the motor to the central shaft, which is securely mounted within a reinforced base to ensure stability and minimal vibration. Attached to the central shaft is a drive beam that spans radially across the circular track and supports the vehicle assemblies at its ends. A transfer plate with a rubber interface connects the beam to the shaft to absorb torsional vibrations and provide mechanical flexibility. The design allows for symmetrical load distribution across the system, and the vertical alignment of the motor ensures minimal lateral deflection during operation.

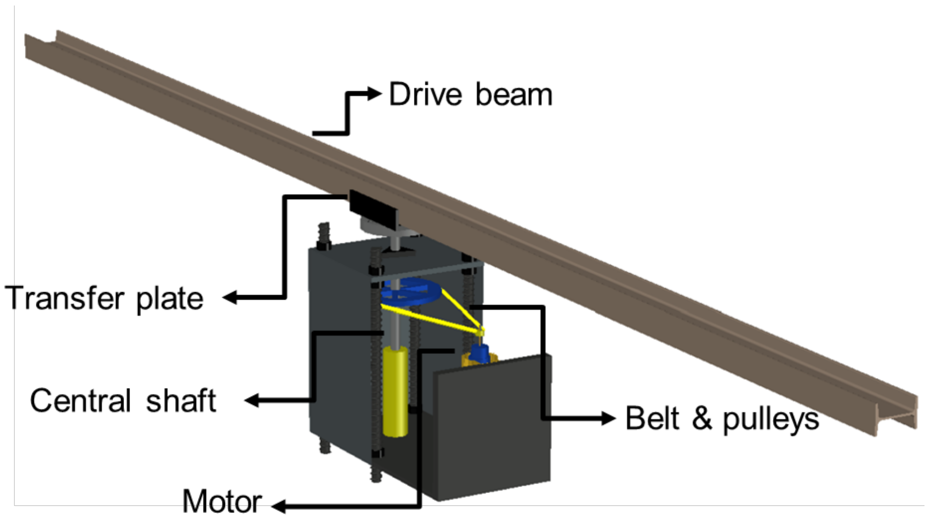

Figure 9: CAD view of the central pivot system

4.2.2.2 Vehicle Assembly

The vehicle assembly replicates the vertical dynamics of the vehicle using a multi-stage suspension system. As shown in **Figure 10**, each assembly includes a flanged wheel that rides on the circular rail, a guide system allows for free vertical and lateral motion, and two concentric suspension layers simulating the primary and secondary suspension systems. The vehicle is composed of a rigid frame that holds stacked weights representing the carbody and bogie masses. These masses are connected using helical compression springs to emulate suspension behavior. The inclusion of both primary and secondary suspensions ensures that the vibrational response of the system can reflect realistic dynamic coupling between train components. Rubber damping pads are also inserted between the stacked masses to replicate damping behavior.

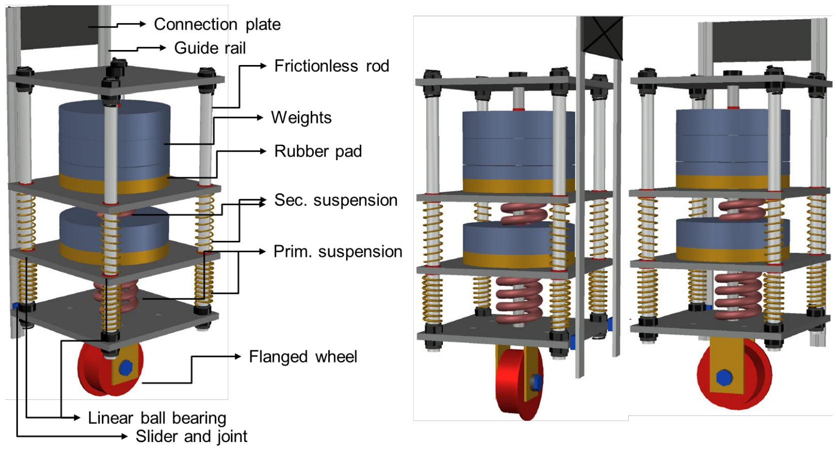

Figure 10: CAD view of the vehicle assembly

4.2.2.3 Track System

The track system, presented in **Figure 11**, consists of multiple curved segments, completing a full 360°. The base layer includes flexible rubber padding, which represents the ballast's deformability and provides tunable vertical support. To simulate different track stiffness profiles, modular inserts, including small springs, soft fillers, or rigid supports can be placed beneath selected sleepers. This allows us to implement various types of stiffness irregularities, such as missing sleepers, suspended segments, or locally reinforced sections. The track structure is also modular enough to accommodate changes in geometry, rail height, or surface profile.

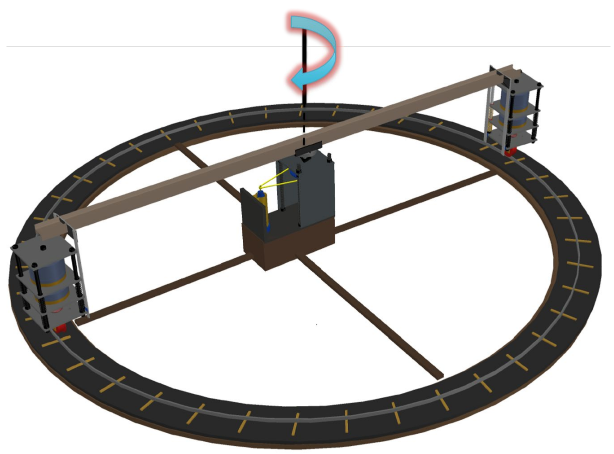

Figure 11: CAD view of the track system

4.2.3 Track–Vehicle Assembly and Actuation System

This lab test rig focused on refining the realism and operational continuity of the system.

As shown in **Figure 12**, the testbed consists of a circular track assembled from 24 G-scale curved rail segments (PIKO 35215), each with a 1240 mm radius. The degree of curvature for each segment is 15°. These segments form a complete ring 2.48 meters in diameter, creating a continuous rolling surface for the scaled vehicle. The rails are mounted on sleepers, which rest on a custom-designed substructure made of rubber pad strips that replicate the compliance of a full-scale ballast layer. To introduce changes in stiffness and simulate irregular support conditions, small springs or fillers can be inserted beneath selected ties. The structure mimics the layered behavior of ballasted tracks and allows experimental control over track properties.

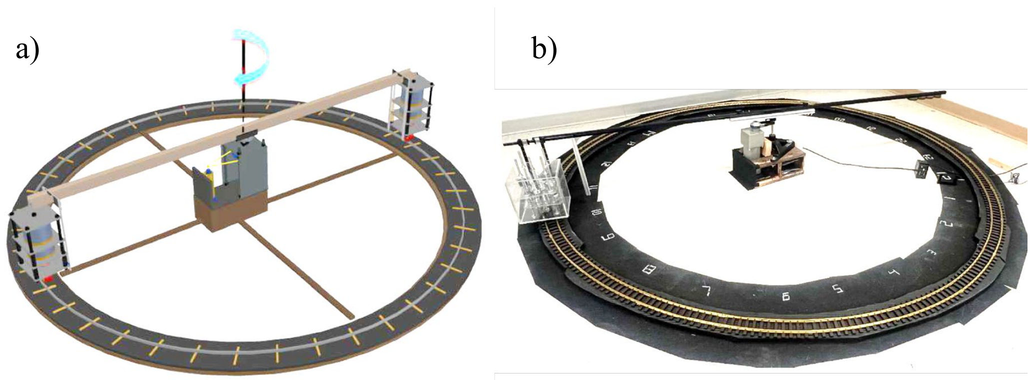

Figure 12: a) CAD view and b) Lab setup of the test rig

The vehicle is actuated by a central rotary drive system, consisting of a 110V, 25W AC gear reduction motor with variable speed control (up to 12 RPM), mounted vertically on a rigid base. The motor drives a central shaft connected to a 2440-millimeter-long aluminum T-slot beam, which extends radially from the center. This drive beam serves as the primary motion delivery mechanism and can support two scaled vehicle assemblies mounted at its ends. The vehicle consists of wheelsets, a box, and a vertical guide system that allows free vertical motion. Springs and dampers can be integrated into the box to approximate the vehicle primary and secondary suspension systems.

4.2.4 Experimental Data Collection and Preliminary Observations

Figure 13 presents representative data collected during the laboratory-scale experiments conducted using the circular test rig. The experiment was designed to evaluate the repeatability and stability of the proposed detection framework under continuous operation and controlled stiffness variation. Data were recorded over five consecutive rotations of the vehicle around the circular track, allowing repeated traversal of the same track segments under identical geometric conditions. The shaded red regions in all plots correspond to track segments with increased stiffness relative to the baseline support condition. **Figure 13** illustrate the travel distance, vehicle speed, and vertical acceleration recorded during the test. The travel-distance plot confirms consistent progression of the vehicle along the track, while the averaged speed profile shown in red demonstrates relatively stable operating conditions with minor fluctuations. The corresponding vertical acceleration signal exhibits nonstationary behavior typical of onboard measurements and does not, by itself, clearly indicate the presence or location of stiffness variations.

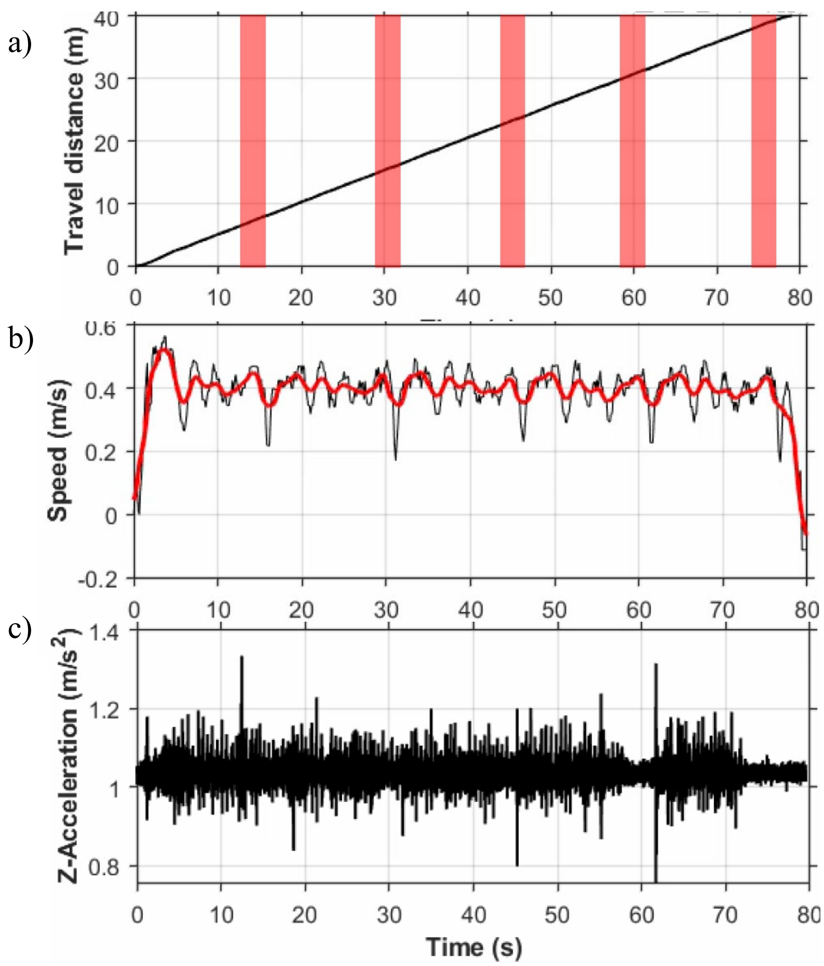

Figure 13: Laboratory-scale experimental data showing a) travel distance, b) vehicle speed, and c) vertical acceleration

Figure 14 presents the instantaneous energy profile derived from the vertical acceleration signal using the proposed multi-stage signal-processing framework. As in the speed profile, the red curve denotes a moving-average representation of the energy signal, included to emphasize the underlying spatial trend. A repetitive and spatially consistent change in instantaneous energy is observed each time the vehicle traverses the stiffened segments, aligning closely with the shaded red zones. As the number of circular passes increases, the contrast between the stiffened segments and the surrounding baseline track becomes increasingly pronounced. This behavior is attributed to a gradual reduction in overall track stability during extended operation, which amplifies the dynamic response differences between regions of differing support stiffness. The moving-average energy trend further highlights this effect by suppressing high-frequency fluctuations and revealing the evolving separation between stiffness zones.

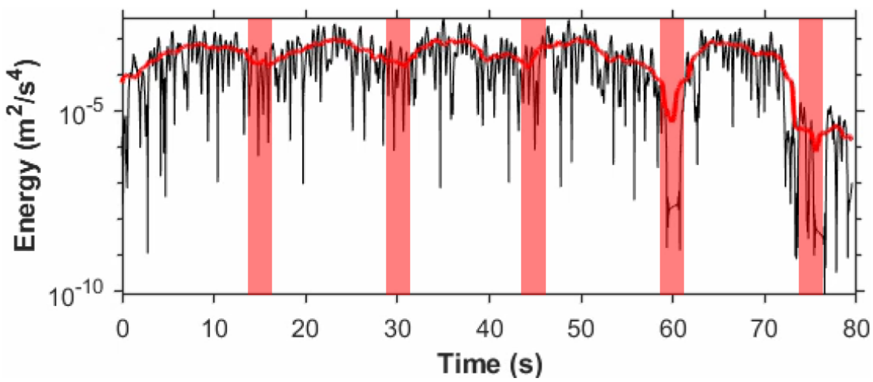

Figure 14: Instantaneous energy derived from vertical acceleration

These preliminary observations demonstrate that, under laboratory-scale conditions and continuous operation, the proposed framework can consistently identify stiffness-induced dynamic signatures aligned with known support variations. While the results are presented at a feasibility level, they provide supporting evidence for the robustness of instantaneous energy as an indicator for detecting localized track stiffness changes in controlled experimental environments.

5 CONCLUSION

This report presents the Year-2 progress toward the development of a scalable, onboard framework for rapid detection of track stiffness changes using in-motion vibration measurements. Building upon the foundational feasibility demonstrated in Year-1, the current effort advanced the methodology through a combination of high-fidelity numerical simulation and controlled laboratory-scale experimentation, providing a more rigorous assessment of system behavior under realistic dynamic conditions.

High-fidelity 3D vehicle–track interaction simulations were used to evaluate the proposed multi-stage, physics-informed signal-processing framework under complex vehicle dynamics, distributed track support conditions, and measured track geometry inputs. The numerical results demonstrated that localized stiffness deficiencies, whether associated with excessive deflection, abrupt sleeper-to-sleeper stiffness transitions, or non-compliant stiffness ranges, produce consistent and spatially localized signatures in the instantaneous energy domain. These findings confirm the sensitivity of the proposed energy-based proxy to a broad range of stiffness-related support conditions. To complement the numerical evaluation, a scaled laboratory experimental platform was developed to assess the framework performance in a physically controlled and repeatable environment. The laboratory experiments demonstrated that stiffness-induced dynamic signatures can be repeatedly identified across multiple vehicle passes, even under continuous operation and evolving track stability conditions. The observed correspondence between known stiffness zones and changes in instantaneous energy further supports the robustness of the proposed approach and its suitability for practical implementation.

Collectively, the Year-2 results establish the technical feasibility of detecting track stiffness changes using onboard vibration data without requiring direct access to the track or service interruption. While the current work focuses on proof-of-concept and feasibility rather than full system optimization, it provides strong evidence that the proposed framework can reliably identify stiffness-related anomalies across multiple modeling fidelities and experimental conditions. Future work will build upon these findings by extending validation to field-based datasets, refining classification and severity-assessment capabilities, and advancing toward real-time, edge-compatible implementation. These next steps will further support the long-term goal of enabling network-scale, data-driven track condition monitoring to inform proactive maintenance and enhance railway safety.

Building on the Year-2 feasibility findings, the planned Year-3 effort will focus on extending the framework toward operational readiness. This work will include field-based validation using in-service data, development of automated classification and severity-assessment strategies, and integration of the detection framework into a real-time, edge-compatible architecture. These activities are intended to transition the methodology from controlled validation to practical deployment, supporting network-scale, data-driven track condition monitoring for proactive maintenance and enhanced railway safety.

6 REFERENCE

[1] W.P. Powrie, Louis Le A Guide to Track Stiffness, 2016.

[2] L. Xu, W. Zhai, A new model for temporal–spatial stochastic analysis of vehicle–track coupled systems, Vehicle System Dynamics, 55 (2017) 427-448.

[3] C. Shi, Y. Zhou, L. Xu, X. Zhang, Y. Guo, A critical review on the vertical stiffness irregularity of railway ballasted track, Construction and Building Materials, 400 (2023) 132715.

[4] T. Sussman, W. Ebersöhn, E. Selig, Fundamental nonlinear track load-deflection behavior for condition evaluation, Transportation Research Record, 1742 (2001) 61-67.

[5] D. Davis, D. Plotkin, Bridge Approaches and Track Stiffness, (2008).

[6] A. Talbot, ASCE-AREA committee on stresses in rail road tracks, first progress report, Proceedings of AREA, 19 (1918).

[7] A.M. Zarembski, J. Choros, On the measurement and calculation of vertical track modulus, (1979).

[8] A.D. Kerr, On the determination of the rail support modulus k, International Journal of Solids and Structures, 37 (2000) 4335-4351.

[9] S. Grassie, S. Cox, The dynamic response of railway track with unsupported sleepers, Proceedings of the Institution of Mechanical Engineers, Part D: Transport Engineering, 199 (1985) 123-136.

[10] M.J. Steenbergen, Physics of railroad degradation: The role of a varying dynamic stiffness and transition radiation processes, Computers & Structures, 124 (2013) 102-111.

[11] R. Naseri, S. Mohammadzadeh, D.C. Rizos, Rail surface spot irregularity effects in vehicle-track interaction simulations of train-track-bridge interaction, Journal of Vibration and Control, (2024) 10775463241232024.

[12] P. Wang, L. Wang, R. Chen, J. Xu, J. Xu, M. Gao, Overview and outlook on railway track stiffness measurement, Journal of Modern Transportation, 24 (2016) 89-102.

[13] M. Oregui, Z. Li, R. Dollevoet, Identification of characteristic frequencies of damaged railway tracks using field hammer test measurements, Mechanical Systems and Signal Processing, 54-55 (2015) 224-242.

[14] C. Norman, S. Farritor, R. Arnold, S. Elias, M. Fateh, M. El-Sibaie, Design of a system to measure track modulus from a moving railcar, US Department of Transportation, Federal Railroad Administration, Office of …, 2006.

[15] M.X.D. Li, E.G. Berggren, A Study of the Effect of Global Track Stiffness and Its Variations on Track Performance: Simulation and Measurement, Proceedings of the Institution of Mechanical Engineers, Part F, 224 (2010) 375-382.

[16] T. Sussmann, D. Read, J. Choros, S.M. Farritor, Gaining Track Support to Improve Track Safety, Efficiency, and the Competitiveness of the Rail Industry, (2013).

[17] M. Brown, D. Li, Ground penetrating radar technology evaluation and implementation: phase 2, United States. Federal Railroad Administration. Office of Research …, 2017.

[18] L. Auersch, Excitation of ground vibration due to the passage of trains over a track with trackbed irregularities and a varying support stiffness, Vehicle System Dynamics, 53 (2015) 1-29.

[19] M. Germonpré, J. Nielsen, G. Degrande, G. Lombaert, Contributions of longitudinal track unevenness and track stiffness variation to railway induced vibration, Journal of Sound and Vibration, 437 (2018) 292-307.

[20] D.C. Rizos, R. Naseri, B.L. Gedney, Rapid Detection of Track Changes from Onboard Data Acquisition Records, University Transportation Center for Railway Safety (UTCRS) Tier-1 …, 2024.

[21] R. Naseri, B.L. Gedney, H. Asgari, D.C. Rizos, Rail squat detection using hybrid processing of axle box acceleration measurements, Results in Engineering, 26 (2025) 105343.

[22] R. Naseri, D.C. Rizos, A Multi-Stage Physics-Informed Signal Processing Framework for In-Motion Detection of Track Stiffness Irregularities Using Onboard Vibration Sensors, Transportation Research Record, (2026).

[23] R. Naseri, B.L. Gedney, D.C. Rizos, Onboard track stiffness variation monitoring using hybrid signal processing techniques, International Heavy Haul Association, 2025.

[24] R. Naseri, Development and Implementation of a multi-stage physics-informed Signal Processing Technique for In-Motion Track Change Detection, University of South Carolina, 2026.

[25] F.R.A. FRA, Automated Track Inspection Program (ATIP) Overview. [online] Available at: https://railroads.dot.gov/railroad-safety/divisions/track/atip-overview, Accessed: Dec. 30, 2025.

[26] R. Naseri, D.C. Rizos, A Multi-Stage Physics-Informed Signal Processing Framework for In-Motion Detection of Track Stiffness Irregularities, Transportation Research Record (2026).

[27] R. Naseri, B.L. Gedney, H. Asgari, D.C. Rizos, A Hybrid Rail Surface Spot Irregularities (RSSI) Detection Algorithm Based on Onboard Measurements, ASME/IEEE Joint Rail Conference, American Society of Mechanical Engineers, 2024, pp. V001T001A010.

[28] D. Rizos, R. Naseri, B. Gedney, Rapid Detection of Track Changes From Onboard Data Acquisition Records, 2024.

[29] Y. Qian, D.C. Rizos, R. Naseri, A. Data, Intelligent Risk Assessment and Prediction System (i-RAPS), United States Department of Transportation, Federal Railroad Administration. Office of Research, Development, and Technology, , 2025.

[30] W.W. Hay, Railroad engineering, John Wiley & Sons, 1991.

[31] A.L. Pita, P.F. Teixeira, F. Robuste, High speed and track deterioration: the role of vertical stiffness of the track, Proceedings of the Institution of Mechanical Engineers, Part F: Journal of Rail and Rapid Transit, 218 (2004) 31-40.

[32] L. Puzavac, Z. Popović, L. Lazarević, Influence of track stiffness on track behaviour under vertical load, Promet-Traffic&Transportation, 24 (2012) 405-412.